

Angewandte Chemie

Near-IR Emitting Ir(III) Complexes with Heteroaromatic β -Diketonate Ancillary Ligands for Efficient Solution Processed OLEDs: Structure-Property Correlations

--Manuscript Draft--

Manuscript Number:	201509798R1
Article Type:	Communication
Corresponding Author:	Alberto Bossi, Ph.D. Istituto di Scienze e Tecnologie dei Materiali del Consiglio Nazionale delle Ricerche Milan, ITALY
Corresponding Author E-Mail:	alberto.bossi@istm.cnr.it;bossi.alb1@gmail.com
Other Authors:	Sagar Kesarkar, Ph.D. Wojciech Mróz, Ph.D. Marta Penconi, Ph.D. Mariacecilia Pasini, PhD Silvia Destri Marco Cazzaniga, PhD Davide Ceresoli, PhD Patrizia Romana Mussini, Associate Professor Clara Baldoli Umberto Giovanella, PhD
Abstract:	Three near-infrared (NIR) emitting neutral Ir(III) complexes based on benzothiophenyl-isoquinoline ligand, Ir(iqbt)2dpm (1), Ir(iqbt)2tta (2) and Ir(iqbt)2dtdk (3), were synthesized and display high luminescence quantum yield (up to 16 %) in the range 680 to 850 nm from a triplet ligand center state (3LC). Photophysical and electrochemical properties of the complexes 1–3 are discussed and supported by computational modelling, establishing the relationship among structure, energy levels and properties. Solution processed phosphorescent organic light-emitting devices (PHOLEDs) were fabricated with the simple architecture ITO/PEDOT:PSS/emitting layer (EML)/Ba/Al. The NIR emitting PHOLEDs reach remarkable external quantum efficiency (EQE) above 3 % (for complex 1) and negligible efficiency roll-off, exceeding the highest values ever reported for solution-processable NIR emitters.
Response to Reviewers:	Answers to the reviewers. The authors thanks the reviewers for their suggestions and comments; all agrees to this revision submitted and to the addition of the two co-authors Marco Cazzaniga and Davide Ceresoli, for the computational work done and interpretations. Review of 201509798 Reviewer 1: 1.1 Q: "NMR typically detects > 5 % impurity but not the low levels that can affect emission spectra. High res mass spec tells you have the compound but it is uninformative as to anything else that is there. It would be good to see microanalysis included in the characterization". A: We added in the supporting information the elemental analysis characterizations. The samples purity was also checked, prior to any device processing by means of HPLC analysis which indicates that the compounds purity titles was above 99%. (S1.1 HPLC-MS analysis) 1.2 Q: I also note that there is no crystallographic data for the materials but I think this is fine; it would be good to have a structure but compounds do not always cooperate in

this regard.

A: Indeed crystallographic information would have been of help, unfortunately, as the reviewer says, we did not get suitable crystal for diffraction studies.

1.3

Q: I note there are quite a few patents with the benzothiophenyl-isoquinoline ligand and iridium (III) I wonder if it is appropriate to reference some of these publications?

A: We added in ref 19b.

S. Tobita, T. Yoshihara, M. Hosaka, T. Takeuchi, Compound and functional luminescent probe comprising the same, 2014, Patent number US 8,623,239 B2 and EP2348314A1, EP2348314A4, US20110201802, WO2010044465A1

We added in the SI, Ref.8:

L. Ying, J. Zou, W. Yang, H. Wu, A. Zhang, Z. Wu, Y. Cao, Macromol. Chem. Phys. 2009, 210, 457–466; S. Tobita, T. Yoshihara, M. Hosaka, T. Takeuchi, Compound and functional luminescent probe comprising the same, 2010, Patent number EP2348314A1; J. Kamatani, S. Okada, A. Tsuboyama, T. Takiguchi, S. Miura, K. Noguchi, T. Moriyama, S. Igawa, M. Furugori, Luminescent element and display, 2002, Patent number WO 2002044189 A1

Reviewer 2:

2.1) The computational procedure and the choice of method/basis set are not well described. On page SI Page 1/2 it is written that 'DFT calculation were performed using the Titan (Wavefunction Inc.) computational package under B3LYP/LACVP** basis set known to provide good fit to the geometric parameters. Ground state geometry were optimised after a fast minimization and orbitals were rendered at 0.03 isodensity unit. The singlet ground state structure was used as input geometry for the triplet state geometry optimization at the B3LYP/LACVP**.'

2.1a)

Q: there is no appropriate reference to the program package

A: we added the requested references for both Titan and Gaussian packages.

2.1b)

Q: LACVP** basis set is an abbreviation existing only in the Titan (Wavefunction Inc.) computational package and is not widely accepted. The LACVP** keyword should indeed be equivalent to a combination of the 6-31G** basis set for H, C, O,N,S with the LANL2DZ effective core basis set for Ir. The authors should edit the sentence and it should contain clear information about the basis set.

A: we added footnotes including the proper description of the basis set for both Titan and Gaussian computations. Ref. 4, 7 and 9

2.1c)

Q: 'B3LYP/LACVP** basis set known to provide good fit to the geometric parameters.' - there is no reference or any kind of confirmation of this statement. Moreover, the authors should look for method/basis set combination that is appropriate for modelling absorption/emission properties of Ir-complexes, rather than just the geometrical parameters. For example, it is well known that some methods/basis set combinations give good results for ground state characteristics but do not work well for absorption/emission properties, especially if the molecules are characterized with charge-transfer excitations.

A: we added reference 6: a) M. J. Jurow, A. Bossi, P. I. Djurovich, M. Thompson, Chem. Mater. 2014, 26(22), 6578–6584. b) A. Bossi, A. F. Rausch, M. Leidl, R. Czerwiniak, M. T. Whited, P. I. Djurovich, H. Yersin, M. E. Thompson, Inorg. Chem. 2013, 52 (21), 12403–12415. c) J. Brooks, Y. Babayan, S. Lamansky, P. I. Djurovich, I. Tsyba, R. Bau, M. E. Thompson, Inorg. Chem. 2002, 41, 3055–3066; d) P. J. Hay, J. Phys. Chem. A, 2002, 106 (8), 1634–1641. T. A. Niehaus, T. Hofbeck, H. Yersin, RSC Adv. 2015, 5, 63318–63329

And ref. 8. A review paper of common practice in TDDFT calculations by experts of the field. C. Adamo and D. Jacquemin, Chem. Soc. Rev. 2013, 42, 845; D. Escudero, D. Jacquemin, Dalton Trans., 2015, 44, 8346; S. Fantacci, F. De Angelis,

2.1d)

Q: Also, 'fast minimization' is quite strange and meaningless expression. What are the convergence criteria and algorithm for optimization that have been used?

A: we specify in the SI. Ground state geometries were optimised first with the semiempirical PM3 model then at the full DFT theory level.

2.1e)

Q: The solvent effects are not taken into account. Their inclusion is required when dealing with solution processed OLED molecules.

A: Typically the solvent effects are included via a PCM method; this would be needed to simulate solvent interaction with the molecules. However, the PCM method could not simulate straightforwardly the solid matrix environment in which the emissive dopant is dispersed into the OLED active layer. In any case, since our reported DFT/TDDFT data already well reproduce the observed trends and evidence the necessary correlation requested, solvents effect are not of paramount importance in this case.

2)

Q: The analysis of the emission/absorption properties of organometallic complexes and the character of their excited states is usually performed in the framework of time-dependent DFT theory (TDDFT). Within the TDDFT theory the authors will be able to theoretically predict the energy of the vertical $S_0 \rightarrow S_n$ and $S_0 \rightarrow T_n$ transitions, the intensity of the $S_0 \rightarrow S_n$ transitions (related to the oscillator strength), as well as all the orbitals involved in these transitions. However, at the moment the authors represent only ground state DFT results, which can be extrapolate to interpret optical properties but are insufficient for the theoretical modelling of the complexes. TDDFT calculations on organometallic complexes with similar molecular size are feasible in respect to computational time and resources and are widely reported in the literature. Therefore, in order to be more convincing, the authors should perform TDDFT calculations and include them in the next version of the paper. For example, just looking at the ground state DFT results it is not clear what is the importance of the low energy metal-to-ligand charge transfer and the dtdk ligand - LUMO density of 1 is iqb based but in 2 and 3 it is betadiketonate based and this suggest some possible differences between the excited states character in 1, 2 and 3 ... and similar open questions that arise from the lack of TD-DFT modelling.

A: the requested TDDFT modeling has been performed and reported extensively in SI while a short description is placed in the main article. the role of LUMO shift onto the diketonate ancillary ligand is discussed

3)

Q: The authors state that in all 1, 2, 3, the emission originates from an iqb 3LC state (Page 2), however the triplet spin density (Figure 3) clearly indicates an important d-coefficient on the metal centre and hence it can be argue if the emission is ligand based. Also, the atomic spin density represent the difference between the electrons with spin up and down, associated with a given atom. Therefore, it has sign -/+. In this sense, the representation the triplet spin density (Figure 3) is not entirely informative. Also, how the SOMO orbitals in the triplet states look like?

A: the attribution of the emissive state has been corrected as "perturbed 3LC/3MLCT type" and the comments about metal participation have been added (also in consideration of Yersin at.al. 2007). We recalculated the spin densities at the unrestricted B3LYP level. In the SI we do not report all the participating SOMOs because the spin density is mostly generated by the highest alpha SOMO. The remaining SOMOs (alpha and beta) contribute to a smaller extent to the spin density.

4)

Q: On Page 1 it is written -"Weak bands in the region of $\lambda > 600$ nm (Figure 1a inset) are assigned to ground state excitation into the lowest triplet state ($S_0 \rightarrow T_1$; Table 1)." Vertical $S_0 \rightarrow T_1$ excitations are spin forbidden. While some authors have reported these types of absorptions, they are extremely weak and often masked by the larger MLCT transitions to the blue. There are clear examples of Pt transitions of this type, but such transitions are not widely accepted and one should take great care in their assignment. Is it really necessary to assign these small intensity peaks? If the authors feel this is an important part of their work than TD-DFT calculations will be very helpful

	<p>in the correct assignment of the transitions.</p> <p>A: it is of importance to understand and assign properly these bands. Their “high” extinction coefficients (for being triplet absorption) is tightly connected to the complexes’ high luminescence quantum efficiency/radiative rates. Now TDDFTs provided clear indications on the origin of the triplet transitions located at low energy, far apart from the singlet MLCT ones. Of course the S0->T1 have vanishing oscillator strength in TDDFT in absence of SOC. With these findings we can safely confirm the statement “Weak bands in the region of $\lambda > 600$ nm (Figure 1a inset) are assigned to ground state excitation into the lowest triplet state (S0 -> T1; Table 1)”.</p> <p>Before the TDDFT studies our interpretation accounts from at least three feature suggesting their origin of S0-T1 type:</p> <ul style="list-style-type: none"> a)Low molar absorptivity b)Almost zero Stokes-shift between these bands and the emission (hence small 0-0 distance) further evident in the 77K data. c)Their vibronic progression (eg. considering for complex 1 the peaks at 687nm and 628nm) mirror the luminescence vibrational peaks with a breathing mode of ca. 1400cm⁻¹ d)In the literature Yersin and coworker (ref, 16 in the manuscript) addressed similar peaks in a closely matching complex (with pyridine instead of quinoline). <p>The experimental results are intriguing ... revisions will be needed for publication in Angewandte Chemie.</p> <p>In conclusion we performed the requested calculation and changes. We found that complete support to the experimental observation is obtained through the TDDFT calculations and the triplet state spin densities properly revised. All the authors agree to this revision and to the addition of the two co-authors Marco Cazzaniga and Davide Ceresoli, for the significant computational work done and interpretations. The uploaded revised manuscript and SI the revisions are highlighted in yellow.</p> <p>Best regards Alberto Bossi</p>
Additional Information:	
Question	Response
Submitted solely to this journal?	Yes
Has there been a previous version?	No
Dedication	

Near-IR Emitting Ir(III) Complexes with Heteroaromatic β -Diketonate Ancillary Ligands for Efficient Solution Processed OLEDs: Structure-Property Correlations

Sagar Kesarkar, Wojciech Mróz, Marta Penconi, Mariacecilia Pasini, Silvia Destri, Marco Cazzaniga, Davide Ceresoli, Patrizia R. Mussini, Clara Baldoli, Umberto Giovanella* and Alberto Bossi*

Abstract: Three near-infrared (NIR) emitting neutral Ir(III) complexes based on benzothiophenyl-isoquinoline ligand, $Ir(iqbt)_2dpm$ (**1**), $Ir(iqbt)_2tta$ (**2**) and $Ir(iqbt)_2dtk$ (**3**), were synthesized and display high luminescence quantum yield (up to 16 %) in the range 680 to 850 nm from a triplet ligand center state (3LC). Photophysical and electrochemical properties of the complexes **1–3** are discussed and supported by computational modelling, establishing the relationship among structure, energy levels and properties. Solution processed phosphorescent organic light-emitting devices (PHOLEDs) were fabricated with the simple architecture ITO/PEDOT:PSS/emitting layer (EML)/Ba/Al. The NIR emitting PHOLEDs reach remarkable external quantum efficiency (EQE) above 3 % (for complex **1**) and negligible efficiency roll-off, exceeding the highest values ever reported for solution-processable NIR emitters.

Driven by military,^[1] civil and telecommunication needs, the development of NIR luminescent materials (emitting beyond 700 nm) has emerged as a promising and challenging research field with potential application in OLEDs, night vision readable displays and bio-imaging.^[1,2]

NIR emitters suitable for OLEDs application have been developed either using pure organic molecules and/or polymers or organometallic compounds.^[3] Late transition metal complexes of the second and third row display high luminescence quantum efficiency (Φ_L) resulting from the strong spin-orbit coupling, due to heavy metal effect, and the intrinsic conformational rigidity. In addition, the ease of engineering their electronic properties make these compounds of particular relevance in NIR applications.^[4] PHOLEDs, which allow the harvest of both singlet and triplet excitons,^[5] have shown record EQE of 9–14.5 % in the 650–800 nm range employing Pt porphyrins or Pt excimers in sophisticated architecture.^[6] However, detrimental efficiency roll-off at increasing current density was observed.^[5a,7] This is primarily ascribed to easy aggregation of square-planar systems and their intrinsic long phosphorescence lifetime. On the other

hand phosphorescent cyclometalated transition-metal complexes (e.g. containing Ir(III),^[8a] Os(II),^[8b] Re(I)^[8c]), having octahedral geometry, have been recently explored to limit the efficiency roll-off issues.

Cao et al. reported Ir(III) based solution processed optimized device with peak emission at 690 nm and EQE over 5 %.^[9] Similarly, Tao et al. demonstrated negligible efficiency roll-off in Ir(III) based devices, obtained by solution or vacuum methods, emitting in the range 700–800 nm with EQE of about 2 %.^[10] The most successful strategy to lower the emission energy of cyclometalated complexes, based on chelating ligand with N^2C donor atoms,^[3c] is a careful expansion of the ligand conjugated system.^[11–13] For instance, over 100 nm red shift can be achieved employing isoquinoline and naphthyl groups instead of pyridine and phenyl ones.^[14,15] As well, the introduction of electron-rich heteroaromatic rings (e.g. thiophene) also serve to the scope.^[16] Alternatively, a significant electronic perturbations can be achieved by ancillary ligands modification.^[17] The introduction of β -diketonate ancillary ligands onto homoleptic tris-cyclometalated Ir(III) complex can induce a slight red-shift (10–15 nm) of the emission as in the case of $Ir(thpy)_2acac$ and $Ir(btpy)_2acac$ compared to fac - $Ir(thpy)_3$ and fac - $Ir(btpy)_3$ respectively ($thpy$: 2-thienylpyridine, $btpy$: benzothiienylpyridine).^[18]

Ikawa et al. recently reported a homoleptic fac - $Ir(iqbt)_3$ ($iqbt$: 1-(benzo[*b*]thiophen-2-yl)-isoquinoline) complex including an electron rich benzothiophene moiety emitting at 690 nm with good efficiency.^[19] Solution processed OLED was fabricated with EQE of 1.4 %.^[19a]

We decided to investigate the family of $Ir(iqbt)_2L$ complexes including three different β -diketonate (L) ancillary ligands with increasing conjugation: 2,2,6,6-Tetramethyl-3,5-heptanedione ($Hdpm$), 2-thienoyltrifluoroacetone ($Htta$) featuring one thiophene group and 1,3-di(thiophen-2-yl)propane-1,3-dione ($Hdtdk$) featuring two thiophene groups. These three ligands allow controlling the sterical hindrance and solubility of the complexes (critical for device's active layer processing) and increasing donor character due to the electron rich thiophene groups. Moreover the possibility of a selective functionalization of the thiophene ring in tta and dtk ligands makes these derivatives even more attractive. With this simple strategy we obtained three new full NIR emitting Ir(III) complexes employed in efficient PHOLEDs with negligible roll-off in unoptimized devices.

The new complexes, **1–3** (Chart 1), were prepared in a two steps process (Scheme S1.2). The intermediate μ -chloro-bridged dimer, $[(iqbt)_2IrCl]_2$, prepared by cyclometalation of $IrCl_3 \cdot nH_2O$ with $Hiqbt$ ligand,^[20a] was reacted with $Hdpm$ in 2-ethoxyethanol as solvent at 110°C in the presence of K_2CO_3 to

Dr. S. Kesarkar, Dr. M. Penconi, Dr. M. Cazzaniga, Dr. D. Ceresoli, Dr. C. Baldoli, Dr. Alberto Bossi
Istituto di Scienze e Tecnologie Molecolari- CNR e SmartMatLab
Center, Via C. Golgi 19, 20133 Milano, Italy
E-mail: alberto.bossi@istm.cnr.it

Dr. W. Mróz, Dr. M. Pasini, Dr. S. Destri, Dr. U. Giovanella
Istituto per lo Studio delle Macromolecole- CNR, Via E. Bassini 15,
20133 Milano, Italy
E-mail: u.giovanella@ismac.cnr.it

Prof. P. R. Mussini
Dipartimento di Chimica, Università degli Studi di Milano, Via Golgi
19, 20133 Milano, Italy
Supporting information for this article is available on the WWW
under <http://XXXXXXXXXXXXXXXXXXXX>

give **1** in 22 % yield.^[20b] A slight modification of this procedure was needed for the synthesis of **2** and **3** which were obtained in 32 % and 24 % yield, respectively (SI).^[20c] All complexes are soluble in common organic solvents.

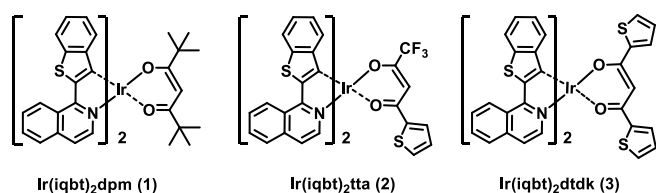


Chart 1. Chemical structures of the complexes 1–3.

For the three complexes in CH_2Cl_2 at 298 K (Table 1 and Figure 1a) the strong absorption in the region below 450 nm underlines a complex spectroscopic admixture of $\pi-\pi^*$ and metal to ligand charge transfer (MLCT) transitions.^[21]

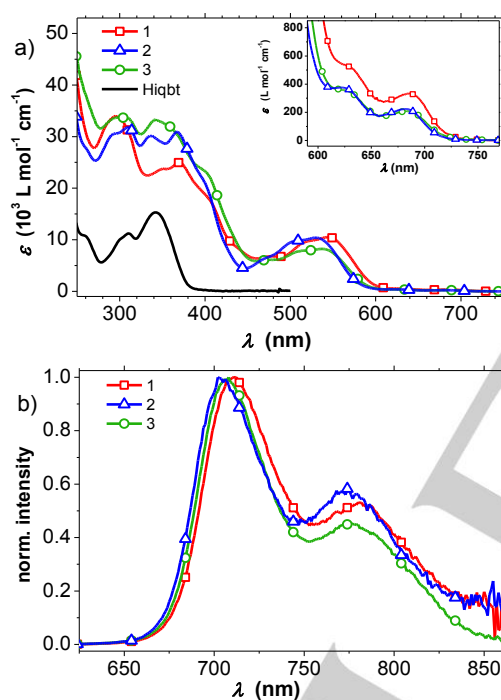


Figure 1. Absorption (a) and emission (b) spectra in CH_2Cl_2 at 298 K of **1** (red squares), **2** (blue triangles) and **3** (green circles); the spectrum of the *Hiqbt* ligand is reported for comparison (black line). The S_0-T_1 absorption transitions are shown in the inset.

The complexes **2** and **3**, compared to **1**, show larger extinction coefficients in the range 350–400 nm due to the overlap of the original diketonate, *Hdtdk* and *Htta*, absorptions.^[22] In the region 450–600 nm the absorption shape of **1**, **2** and **3** is similar and undergoes an hypsochromic shift in the sequence **1**, **3**, **2**. Since the ligands (*iqbt* and diketonates) do not absorb in that region, we assign these bands to $^1,^3\text{MLCT}$ ($d-\pi^*$) transitions due to the coordination of Ir(III) with *iqbt*. Weak bands in the region of $\lambda > 600$ nm (Figure 1a inset) are assigned to ground state excitation into the lowest triplet state ($S_0 \rightarrow T_1$; Table 1 and see TDDFT).^[16] The complexes **1**, **2** and **3** display a structured NIR phosphorescence emission at 710, 704 and 707 nm,

respectively, at 298 K in degassed CH_2Cl_2 solution (Table 1 and Figure 1b). Because of the non-emissive character of *dpm* ligand and the high triplet energy (E_T) of *dtdk* and *tta* (peaked at 531 nm and 502 nm)^[16] compared to the *Hiqbt* one (580 nm, Figure S2.5), the emissions of **1–3** originate from a perturbed *iqbt* based state of $^3\text{LC}^3\text{MLCT}$ character (see DFT calculations Figure 3 and SI section 4). Whereas the phosphorescence emissions of **1–3** slightly shift mirroring the absorption behavior, the excited state dynamic of the complexes are clearly affected by the diketonate structure. The complexes **1** and **3** show almost identical Φ_L (0.16 and 0.14, respectively) and lifetimes (1.40 μs and 1.44 μs) while a two-fold decrease is observed for **2** ($\Phi_L = 0.07$ and $\tau = 0.72 \mu\text{s}$). Radiative rate constants (k_r) are identical, and high, for the three complexes (ca. $1 \times 10^5 \text{ s}^{-1}$ in accordance with the large ϵ of the $S_0 \rightarrow T_1$ transition) while the nonradiative rate (k_{nr}) for **2** is two times larger with respect to **1** and **3**. A minor rigidochromic blue shift is observed at 77 K in 2-MeTHF matrix (Figure S2.6 and Table 1) while the lifetimes increase up to about 2 μs for all the complexes. This evidence suggests the presence of competitive, thermally activated (TA), non radiative deactivation path in **2** that sidesteps the vibrational coupling path to the ground state also present in **1** and **3**.

To elucidate the shift of $^1,^3\text{MLCT}$ bands and the different decay dynamics, we performed electrochemical studies and determined the frontier orbital energy levels. Data were further used in the choice of OLED hosts.

In the cyclic voltammograms, a reversible oxidation peak is observed at +0.38 V, +0.54 V and +0.43 V vs Fc^+/Fc for **1**, **2** and **3** respectively (Figures 2 and S3.1), attributed to a predominantly metal centred process also involving the cyclometalated benzo-thiophene moiety^[23] as evidenced by the DFT calculations (Figures 3 and S4.1).

The anodic shift in oxidation (HOMO level stabilization) of **3** (0.05 eV) compared to **1** may result from the larger π -back-bonding from the Ir(III) centre to the *dtdk* ligand due to the more extended conjugation of the diketonate itself.^[24] In comparison to **1**, the stronger anodic shift of **2** (0.16 eV) results from the combined effects of π -back-bonding (in analogy to **3**) enhanced by the electron withdrawing effect of the CF_3 group on the *tta* moiety. No further oxidation is observed for **1**, whereas a second irreversible oxidation peak at +0.92 V for **3** and at +1.02 V for **2** is assigned to the electrochemical processes on the thiophene unit of the diketonate ligand.

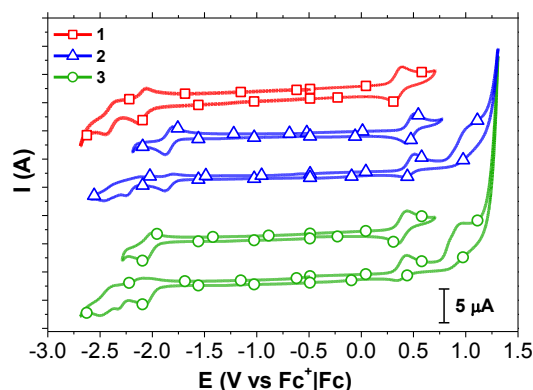


Figure 2. Cyclic voltammograms of the complexes **1–3** recorded vs Fc^+/Fc in DMF at 298 K under N_2 atmosphere (scan rate: 100 mV s^{-1}).

Table 1. Photophysical properties of the complexes 1-3.

	Absorption		Errison 298 K ^[a]				Emission 77 K ^[c]		Electrochemistry ^[d]			
	λ_{abs} (nm) (ϵ (10 ³ L mol ⁻¹ cm ⁻¹) ^[a]	$E_g^{\text{OPT}[b]}$ (eV)	λ_{em} (nm)	τ (μ s)	Φ_L	k_r (10 ⁵ s ⁻¹)	k_{nr} (10 ⁵ s ⁻¹)	λ_{em} (nm)	τ (μ s)	HOMO (eV)	LUMO (eV)	E_g^{EC} (eV)
1	545 (10.5)(MLCT) 687 (0.34)(S ₀ -T ₁)	2.27	710	1.40	0.16	1.1	6.0	694	2.04	-5.15	-2.71	2.44 (2.29) ^[e]
2	528 (10.4) (MLCT) 681 (0.23) (S ₀ -T ₁)	2.35	704	0.72	0.07	0.92	13.0	691	2.03	-5.31	-2.96	2.35 (2.07) ^[e]
3	539 (8.2) (MLCT) 687 (0.21) (S ₀ -T ₁)	2.30	707	1.44	0.14	0.97	6.0	694	2.00	-5.19	-2.76	2.43 (2.25) ^[e]

^[a] N₂ saturated CH₂Cl₂ solutions (C_M ≈ 2 × 10⁻⁵ mol L⁻¹) at 298 K. Radiative k_r and nonradiative k_{nr} rate constants are calculated using the equations $k_r = \Phi_L/\tau$ and $k_{nr} = 1/\tau - k_r$ on the assumption $\Phi_{\text{ISC}} = 1$. ^[b] calcd. at $\lambda_{\text{abs,MLCT}}$. ^[c] In 2-MeTHF frozen matrix at 77 K. Φ_L luminescence quantum yield; τ luminescence lifetime. ^[d] calcd. from E⁰ potentials. ^[e] calcd. from onset criterion (Table S3.1)

Two reversible reduction peaks are observed for **1** at - 2.12 V and - 2.43 V, and can be attributed to two subsequent one-electron reductions localized on isoquinoline moiety.^[25] Complexes **2** and **3** show three reduction peaks. The first one-electron reversible reduction peak locates at -1.87 V for **2** and - 2.07 V for **3**, anodically shifted compared to **1** by 0.25 V and 0.05 V, respectively. The next two, quasi-reversible, reductions are detected below - 2.3 V. Hence, electrochemical HOMO-LUMO gap (E_g^{EC}) follows the order **2**<**3**<**1** contrary to the observed optical gap (E_g^{OPT} are ordered **1**<**3**<**2**).

In contrast, the same energy trend is found comparing E_g^{OPT} and CV gaps of **2** and **3** calculated between first oxidation and second reduction peaks (Table S3.1), suggesting that the first reduction process would involve orbitals on the diketonate *dtdk* and *tta*.^[26]

In agreement, DFT calculations show a large LUMO density distribution on the diketonate ligand in case **2** and **3** in contrast to the *iqbt* localized LUMO in **1** (Figures 3 and S4.1). Hence, the next two cathodic reductions of **2** and **3** are attributed to *iqbt* localized processes; compared to the analogue processes in **1**, their cathodic potentials shift (level destabilization) indicates a partial electronic communication of LUMO and the adjacent LUMO+1 and LUMO+2. Pictorially we observe the LUMO+1 density spreading on *iqbt* but also onto the *tta/dtdk* ligand in **2** and **3**.^[25]

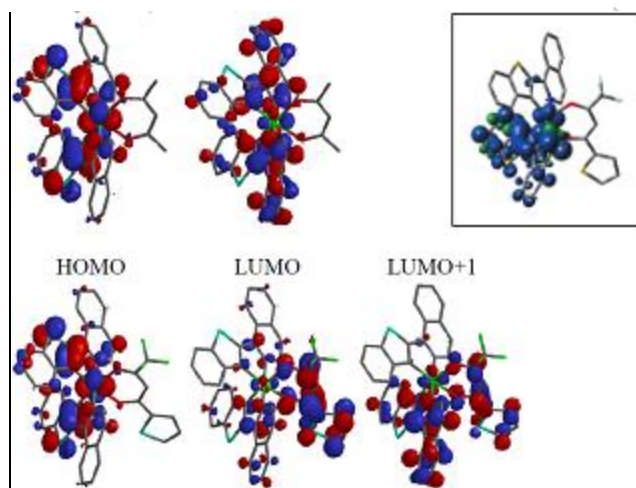


Figure 3. DFT B3LYP/LACVP** frontier orbital counterplot (optimized ground state) of **1** (top) and **2** (bottom) and triplet spin density of **2** (boxed) in the optimized triplet state.

Time-dependent DFT (TD-DFT) calculations were performed to further confirm the electronic transitions described (simulated spectra are reported in Figure S4.3 whereas Table S4.1 summarize the main transitions and the orbital analysis).

The calculated lowest triplet transitions (S₀-T₁) are in the range 724-718 nm following the experimental trend. In **1** the lowest singlet transitions (557 and 545 nm) share a HOMO-LUMO and HOMO-LUMO+1 character. In agreement with the absorptions trend, an hypsochromic shift to 537 nm in **2** and to 543 nm in **3** is observed and differently from **1** these transitions are HOMO to LUMO+2.

Within this energetic framework the non radiative TA path that quenches the emission of **2** could involve population of a low lying Metal Ligand to Ligand' CT state of HOMO to LUMO character which (according to the CV onset gap of 2.07 eV) sits only 0.25 eV above the emissive ³LC/³MLCT state (at 1.79 eV, equivalent to 691 nm peak emission).

A further confirmation arise from TDDFT calculations in which for both **2** and **3** a weak singlet transition of HOMO to LUMO character is found respectively at 586 nm and 572 nm emphasizing the importance of the LUMO shift onto the *tta/dtdk*. Therefore the smaller calculated singlet-triplet gap in **2** and **3**, compared to **1** would justify the higher quenching rate which is at least observed in **2**.

The novel soluble NIR emitters, were tested in solution processed devices with simple architecture ITO/PEDOT:PSS (50 nm)/ PVK (65%):OXD7 (30%):Ir complex (5%) (180 nm)/Ba (7 nm)/Al (100 nm).^[27] Thanks to the suitable choice of PVK as host, efficient emission in the spectral range 680–900 nm is observed for all the devices.

Electroluminescence (EL) spectra (Figure 4a) resemble very well those registered for the complexes in CH₂Cl₂ (Figure 1b), with a peak emission at 714 nm for **1** and **3**, and 709 nm for **2**, and negligible contribution from the matrix. However emission spectra (Figure S5.3) of the devices reveal weak PVK contribution at 420 nm, suggesting that charge trapping mechanism is responsible for EL, facilitated by the position of HOMO and LUMO energies of the emitters with respect to the matrix energy levels (inset Figure 4a).

The PHOLED based on **1** shows a remarkable total EQE of 3.07 % at 1 mA/cm². For **3** and **2** the efficiencies are 2.44 % and 1.28 %, respectively mirroring the Φ_L trend in solution. The devices switch on at 13–15 V (Figure S5.1) and the EQEs remain indeed constant in the radiance (L_e) range 0.1–1 W sr⁻¹ m² (Table 2, Figure 4b).

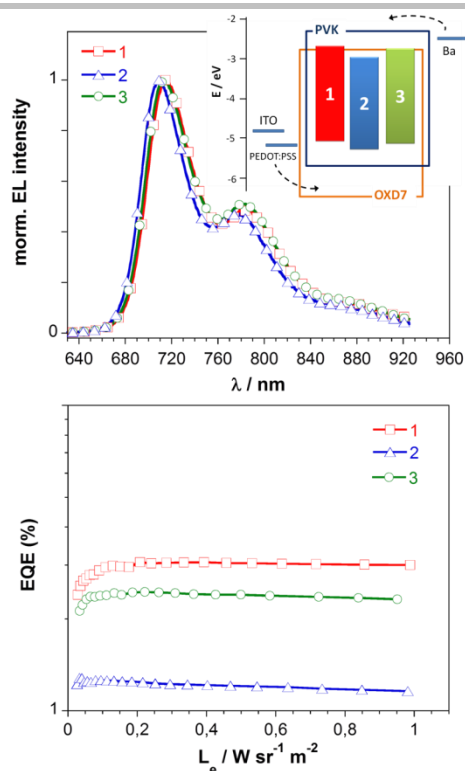


Figure 4. EL spectra (a) and EQE versus radiance (b) for PHOLEDs based on the complexes 1–3. Flat-band energy level diagram of the devices (inset).

Therefore the device efficiency roll-off at high brightness, ascribed to triplet-triplet annihilation or triplet-polaron quenching,^[26] is negligible for **1** and **3** emitters and only moderate (about 10%) for **2**, resulting from the short radiative lifetime and reduced aggregation of the complexes. In complex **2** electron-trapping on the lower LUMO could enhance the EQE decreasing.

Table 2. Characteristics of the devices based on 1–3.

	$\lambda_{\max}^{\text{EL}}$ (nm)	d (nm)	V_{on} (V)	$\text{EQE}_{\text{tot}}^{\text{max}}$ (%)	L_e^{max} ($\text{W sr}^{-1}\text{m}^{-2}$)
1	714	233	13	3.07	1.43
2	709	235	15	1.28	3.1
3	714	234	14	2.44	4.9

In conclusion, we prepared three cyclometalated Ir(III) complexes, with differently engineered β -diketonate ligands, characterized by an efficient and fully NIR emission. Electrochemical and photophysical characterizations, supported by DFT computations, allowed correlating structure-property effects as consequence of the LUMO levels alteration due to the change in the diketonate structure. Unoptimized devices were fabricated to test the ligand effect on the electro-optical properties. The PHOLED based on emitter **1** showed a remarkable EQE of 3.07 %, in a single layer architecture and negligible efficiency roll-off, which is a key feature for technological applications. These devices rank among the most efficient reported employing a truly NIR emitting phosphorescent complex.

Acknowledgements

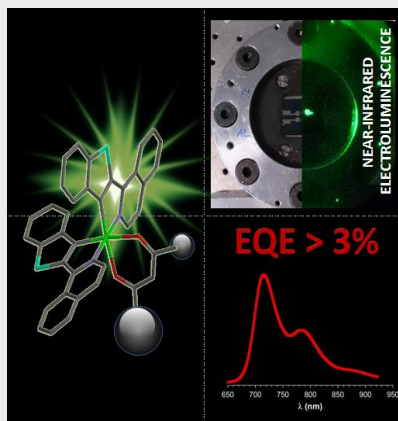
We thank for the financial support Regione Lombardia (decreto 3667/2013) project "Tecnologie e materiali per l'utilizzo efficiente dell'energia solare" and Progetto Integrato Regione Lombardia and Fondazione CARIPOLO (decreti 12689/13, 7959/13), Azione 1 e 2, "SmartMatLab centre". The authors acknowledge Dr. Fausto Cargnoni for useful discussions on TDDFT experiments.

Keywords: near-infrared phosphorescence • optoelectronic materials • photophysics • electrochemistry • DFT calculations • PHOLEDs

- [1] J. Heerlein, M. Behringer, C. Jäger, "Near-infrared power LED for emerging security and defence applications", *Proc. SPIE* 8186, Electro-Optical Remote Sensing, Photonic Technologies, and Applications V, 81860O (October 05, 2011); doi:10.1117/12.897992.
- [2] G. Qian, Z. Y. Wang, *Chem Asian J.* **2010**, 5, 1006-1029; H. Xu, R. Chen, Q. Sun, W. Lai, Q. Su, W. Huang, X. Liu, *Chem Soc. Rev.* **2014**, 43, 3259-3302.
- [3] a) J. Kido, *Chem Rev.* **2002**, 102, 2357-2368; b) T. T. Steckler, O. Fenwick, T. Lockwood, M. R. Andersson, F. Cacialli, *Macromol. Rapid Commun.* **2013**, 34, 990-996; c) H. Xiang, J. Cheng, X. Ma, X. Zhou, J. J. Chruma, *Chem Soc. Rev.* **2013**, 42, 6128-6185.
- [4] W. Y. Wong, *Organometallics and Related Molecules for Energy Conversion, Green Chemistry and Sustainable Technology* (Ed. W. Y. Wong), Springer, 2015.
- [5] a) M. A. Baldo, D. F. O'Brien, Y. You, A. Shoustikov, S. Sibley, M. E. Thompson, S. R. Forrest, *Nature* **1998**, 395, 151-154; b) Y. Sun, N. C. Giebink, H. Kanno, B. Ma, M. E. Thompson, S. R. Forrest, *Nature* **2006**, 440, 908-912;
- [6] a) K. R. Graham, Y. Yang, J. R. Sommer, A. H. Shelton, K. S. Schanze, J. Xue, J. R. Reynolds, *Chem Mater.* **2011**, 23, 5305-5312; b) J. Kalinowski, V. Fattori, M. Cocchi, J. A. G. Williams, *Coord. Chem Rev.* **2011**, 255, 2401-2425 and ref. 87 therein.
- [7] C. Murawaski, K. Leo, M. C. Gather, *Adv. Mater.* **2013**, 25, 6801-68.
- [8] a) Q. L. Xu, X. Liang, S. Zhang, Y. M. Jing, X. Liu, G. Z. Lu, Y. X. Zheng, J. L. Zuo, *J. Mater. Chem. C*, **2015**, 3, 3694-3701; L. Han, D. Zhang, J. Wang, Z. Lan, R. Yang, *Dyes and Pigments*, **2015**, 113, 649-654; b) C. Lee, J. Y. Hung, Y. Chi, Y. M. Cheng, G. H. Lee, P. T. Chou, C. C. Chen, C. H. Chang, C. C. Wu, *Adv. Funct. Mater.* **2009**, 19, 2639-2647; c) X. Li, D. Zhang, H. Chi, G. Xiao, Y. Dong, S. Wu, Z. Su, Z. Zhang, P. Lei, Z. Hu, W. Li, *Appl. Phys. Lett.* **2010**, 97, 263303-3.
- [9] X. Cao, J. Miao, M. Zhu, C. Zhong, C. Yang, H. Wu, J. Qin, Y. Cao, *Chem. of Materials*, **2015**, 27, 1, 96-104.
- [10] a) R. Tao, J. Qiao, G. Zhang, L. Duan, C. Chen, L. Wang, Y. Qiu, *J. Mater. Chem. C* **2013**, 1, 6446-6454; b) R. Tao, J. Qiao, G. Zhang, L. Duan, L. Wang, Y. Qiu, *J. Phys. Chem. C* **2012**, 116, 11658-11664.
- [11] M. E. Thompson, P. I. Djurovich, S. Barlow, S. R. Marder, *In Comprehensive Organometallic Chemistry*; Vol. 12, (Ed. D. O'Hare), Elsevier, Oxford, **2007**, pp 101-194.
- [12] A. Bossi, A. F. Rausch, M. Leitl, R. Czerwieniec, M. T. Whited, P. I. Djurovich, H. Yersin, M. E. Thompson, *Inorg. Chem* **2013**, 52 (21), 12403-12415.
- [13] C.-L. Ho, H. Li, W.-Y. Wong, *J. Organomet. Chem.* **2014**, 751, 261-285.
- [14] J. Brooks, Y. Babayan, S. Lamansky, P. I. Djurovich, I. Tsyba, R. Bau, M. E. Thompson, *Inorg. Chem* **2002**, 41, 3055-3066.
- [15] H. Yersin, *In Highly Efficient OLEDs with Phosphorescent Materials* (Ed. H. Yersin), Wiley-VCH, Weinheim, 2007.
- [16] W. J. Finkenzeller, T. Hofbeck, M. E. Thompson, H. Yersin, *Inorg. Chem* **2007**, 46, 5076-5083.
- [17] B. J. Powell, *Coord. Chem Rev.* **2015**, 295, 46-79.
- [18] a) A. Tsuboyama, H. Iwawaki, M. Furugori, T. Mukaide, J. Kamatani, S. Igawa, T. Moriyama, S. Miura, T. Takiguchi, S. Okada, M. Hoshino, K. Ueno, *J. Am Chem Soc.* **2003**, 125, 12971-12979; b) S. Lamansky, P. Djurovich, D. Murphy, F. Abdel-Razzaq, Hae-Eun Lee, C. Adachi, P. E. Burrows, S. R. Forrest, M. E. Thompson, *J. Am Chem Soc.* **2001**, 123, 4304-4312.

- 1
2
3
4
5
6
7
8
9
10
11
12
13
14
15
16
17
18
19
20
21
22
23
24
25
26
27
28
29
30
31
32
33
34
35
36
37
38
39
40
41
42
43
44
45
46
47
48
49
50
51
52
53
54
55
56
57
58
59
60
61
62
63
64
65
- [19] a) S. Ikawa, S. Yagi, T. Maeda, H. Nakazumi, H. Fujiwara, S. Koseki, Y. Sakurai, *Inorg. Chem. Comm.* **2013**, *38*, 14–19; b) S. Tobita, T. Yoshihara, M. Hosaka, T. Takeuchi, *Compound and functional luminescent probe comprising the same*, **2014**, Patent number US 8,623,239 B2
- [20] a) M. Nonoyama, *Bull. Chem. Soc. Jpn.* **1974**, *47*, 767-768; b) S. Lamansky, P. Djurovich, D. Murphy, F. Abdel-Razzaq, R. Kwong, I. Tsyba, M. Bortz, B. Mui, R. Bau, M. E. Thompson, *Inorg. Chem.* **2001**, *40*, 1704-1711; c) T. Yu, S. Yang, J. Meng, Y. Zhao, H. Zhang, D. Fan, X. Han, Z. Liu, *Inorg. Chem. Comm.* **2011**, *14*, 159-161.
- [21] G.-N. Li, Y. Zou, Y.-D. Yang, J. Liang, F. Cui, T. Zheng, H. Xie, Z.-G. Niu, *J. Fluoresc.* **2014**, *24*, 1545-1552.
- [22] C. Freund, W. Porzio, U. Giovanella, F. Vignali, M. Pasini, S. Destri, A. Mech, S. Di Pietro, L. Di Bari, P. Mineo, *Inorg. Chem.* **2011**, *50*, 5417-5429.
- [23] K. R. J. Thomas, M. Velusamy, J. T. Lin, C. H. Chien, Y. T. Tao, Y. S. Wen, Y. H. Hu, P. T. Chou, *Inorg. Chem.* **2005**, *44*, 5677-5685.
- [24] M. K. Nazeeruddin, R. Humphry-Baker, D. Berner, S. Rivier, L. Zuppiroli, M. Graetzel, *J. Am. Chem. Soc.* **2003**, *125*, 8790-8797.
- [25] S. Ikawa, S. Yagi, T. Maeda, H. Nakazumi, H. Fujiwara, S. Koseki, Y. Sakurai, *Inorg. Chem. Comm.* **2013**, *38*, 14-19.
- [26] K. Beydoun, M. Zaarour, J. A. Gareth Williams, T. Roisnel, V. Dorcet, A. Planchat, A. Boucekkine, D. Jacquemin, H. Doucet, V. Guerschais, *Inorg. Chem.* **2013**, *52*, 12416-12428.
- [27] PVK is polyvinylcarbazole, while OXD-7 is 1,3-bis(5-(4-tert-butylphenyl)-1,3,4-oxadiazol-2-yl)benzene used as additive to improve charges balance within the EML. See as example W. Mróz, R. Ragni, F. Galeotti, E. Mesto, C. Botta, L. De Cola, G.M. Farinola, U. Giovanella, *J. Mater. Chem. C*, **2015**, *3*, 7506-7512.
- [28] S. Reineke, K. Walzer, K. Leo, *Phys. Rev. B*, **2007**, *75*, 125328.

1 Heteroleptic benzo[b]thiophenyl-
2 isoquinolinolate Ir(III) complexes with
3 three diketonate ancillary ligands of
4 increasing conjugation ($\text{Ir}(\text{iqbt})_2\text{L}$) are
5 prepared. Full NIR emission is
6 displayed with the highest emission
7 quantum yield of 16% ($\tau = 1.4\mu\text{s}$ at
8 $\lambda_{\text{max}}=710\text{nm}$). Remarkable high (EQE)
9 above 3 % and negligible efficiency
10 roll-off is found in solution processed
11 OLEDs, employing PVK(65%):
12 OXD7(30%): $\text{Ir}(\text{iqbt})_2\text{L}$ (5%) as
13 emitting layer




Sagar Kesarkar, Wojciech Mróz, Marta Penconi, Mariacecilia Pasini, Silvia Destri, Marco Cazzaniga, Davide Ceresoli, Patrizia R. Mussini, Clara Baldoli, Umberto Giovanella,* and Alberto Bossi*

Page No. – Page No.

Near-IR Emitting Ir(III) Complexes with Heteroaromatic β -Diketonate Ancillary Ligands for Efficient Solution Processed OLEDs: Structure-Property Correlations

14
15
16
17
18
19
20
21
22
23
24
25
26
27
28
29
30
31
32
33
34
35
36
37
38
39
40
41
42
43
44
45
46
47
48
49
50
51
52
53
54
55
56
57
58
59
60
61
62
63
64
65



Click here to access/download

Supporting Information

SI_NIR Emitters_Bossi_Giovanella_ANIE REV 16-12-
15.doc



Click here to access/download
Native Chemdraw files
Chart 1.cdx





Click here to access/download
Additional Material - Author
Fig 1a.eps





Click here to access/download
Additional Material - Author
Fig 1a.opj





Click here to access/download
Additional Material - Author
Fig 1b.eps





Click here to access/download
Additional Material - Author
Fig 1b.opj





Click here to access/download
Additional Material - Author
Fig 2.opj

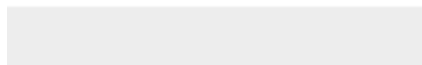




Click here to access/download

Additional Material - Author

Fig 3 new.eps

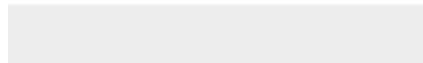


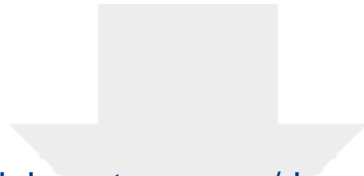


Click here to access/download

Additional Material - Author

Fig 3 new.tif

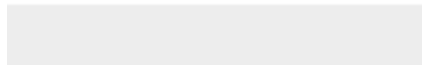


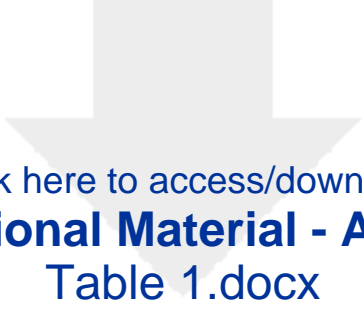


Click here to access/download

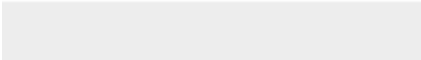
Additional Material - Author

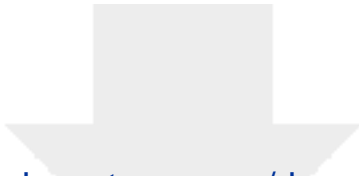
Figure 4 300dpi CYMK.eps



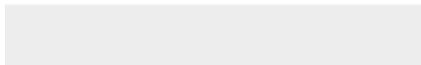


Click here to access/download
Additional Material - Author
Table 1.docx





Click here to access/download
Additional Material - Author
Table 2.docx





Click here to access/download
Additional Material - Author
Fig 2.eps

